

Total Gamma Absorption in Be^9 , O^{16} , F^{19} , and Al^{27} at 20 MeV*

GEORGE TESSLER† AND W. E. STEPHENS

Physics Department, University of Pennsylvania, Philadelphia, Pennsylvania

(Received 14 February 1964)

The total gamma absorption cross section has been measured for Be^9 from 20.04 to 21.24 MeV, O^{16} from 20.37 to 22.04 MeV, F^{19} from 19.97 to 20.46 MeV, and Al^{27} from 20.37 to 20.88 MeV using monochromatic gamma rays from the $\text{T}^3(p,\gamma)\text{He}^4$ reaction. The Be^9 nuclear cross section showed structure at 20.47 ± 0.04 MeV and 20.73 ± 0.04 MeV with integrated cross sections of 0.45 and 0.90 MeV-mb, respectively. The O^{16} nuclear cross section contained a broad peak at 21.02 ± 0.04 MeV with an integrated cross section of 10.4 MeV-mb. There is some indication that this peak is composed of two narrower peaks at about 20.86 and 21.05 MeV. There is also some indication of structure at 20.62 MeV. Above about 21.6 MeV, the O^{16} cross section is rising sharply, consistent with the giant resonance peak above 22 MeV. The F^{19} cross section has a peak at 20.09 ± 0.05 MeV with an integrated cross section of 3.5 MeV-mb. The Al^{27} cross section showed no structure in the energy region investigated.

INTRODUCTION

RECENT experiments¹ of the photonuclear reaction in light nuclei in the giant resonance region indicate more complexity than previously thought. Since most of these experiments have measured partial cross sections, it seems of basic theoretical interest to also examine the total photonuclear absorption cross section. Monochromatic detectors in conjunction with bremsstrahlung radiation have been used for this purpose,² but with poor energy resolution. The Compton magnetic spectrometer employed by Miklavzic *et al.*,² for example, has an energy resolution of about 240 keV. Positron annihilation radiation has also been used, but this method also has a limited energy resolution.³

The present experiment makes use of photons from the $\text{T}^3(p,\gamma)\text{He}^4$ reaction and is an extension of the earlier work of Wolff and Stephens⁴ and Carroll and Stephens.⁵ The advantages of this reaction are that it provides a monochromatic beam of photons with very good energy resolution (about 40 keV in this experiment) and the absolute energy of the photons is known to high accuracy. Although this reaction is a low intensity source of photons, it has been found practical to use it to carry out total absorption measurements, at least over a limited energy range.

THE EXPERIMENT

The total absorption of gamma rays by Be^9 , O^{16} , F^{19} , and Al^{27} was measured using monochromatic gamma rays from the $\text{T}^3(p,\gamma)\text{He}^4$ reaction. Proton beam currents of up to about 30 μA were obtained from the

half-energy section of the University of Pennsylvania Tandem Accelerator. The proton beam was analyzed by a 90° bending magnet whose field strength was measured with a proton magnetic resonance probe. The magnet was calibrated by observing several (p,n) thresholds. The thresholds used were $\text{T}^3(p,n)\text{He}^3$ at 1.0197 MeV,⁶ $\text{Li}^7(p,n)\text{Be}^7$ at 1.8805 MeV⁷ and $\text{C}^{13}(p,n)\text{N}^{13}$ at 3.2373 MeV.⁸

The arrangement of the counters and absorbers is shown schematically in Fig. 1. The counters, consisting of four NaI(Tl) crystals⁹ each 3 in. in diameter by 4 in. in length, were placed symmetrically about a tritium-zirconium target and at 96° to the direction of the proton beam. Each crystal together with a Dumont-6363 photomultiplier tube was sealed in a low-mass light-tight unit (type 12S of the Harshaw integral line). Absorbers were suspended by thin wires between the target and two of the crystals. The other two crystals

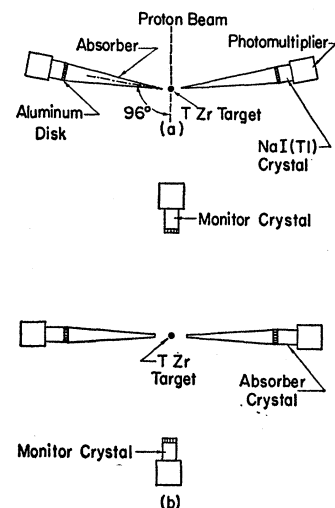


FIG. 1. Arrangement of counters and absorbers relative to target. (a) Section through beam line. (b) Section perpendicular to beam line through target.

* Supported by the National Science Foundation.

† Present address: Westinghouse Electric Corporation, Bettis Atomic Power Laboratory, Pittsburgh, Pennsylvania.

¹ E. Hayward, *Rev. Mod. Phys.* **35**, 324 (1963).

² U. Miklavzic, N. Bezic, D. Jamnik, G. Kernel, Z. Milavc, and J. Snajder, *Nucl. Phys.* **31**, 570 (1962); N. A. Burgov, G. V. Danilyan, B. S. Dolbilkin, L. E. Lazareva, and F. A. Nikolaev, *Zh. Eksperim. i Teor. Fiz.* **43**, 70 (1962) [English transl.: *Soviet Phys.—JETP* **16**, 50 (1963)].

³ C. Schuhl, and C. Tzara, *Nucl. Instr. Methods* **10**, 217 (1961).
⁴ C. P. Jupiter, N. E. Hansen, R. E. Shafer, and S. C. Fultz, *Phys. Rev.* **121**, 866 (1961).

⁵ M. M. Wolff and W. E. Stephens, *Phys. Rev.* **112**, 890 (1958).

⁶ E. E. Carroll and W. E. Stephens, *Phys. Rev.* **118**, 1256 (1960).

⁶ R. O. Bondelid, J. W. Butler, C. A. Kennedy, and A. Del Callar, *Phys. Rev.* **120**, 887 (1960).

⁷ A. Rytz, H. H. Staub and H. Winkler, *Helv. Phys. Acta* **34**, 960 (1961).

⁸ R. O. Bondelid and C. A. Kennedy, *Phys. Rev.* **115**, 1601 (1959).

⁹ Manufactured by the Harshaw Chemical Company, Cleveland, Ohio.

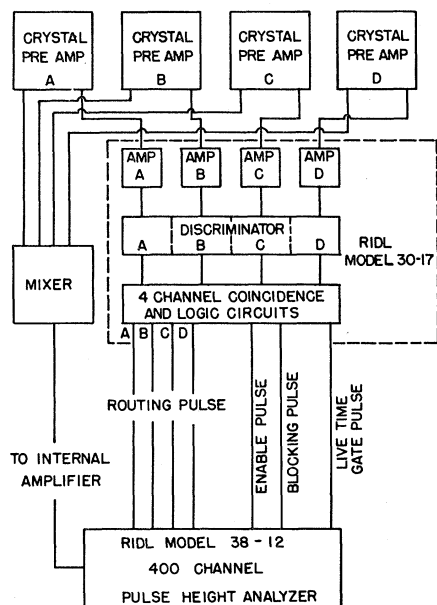


Fig. 2. Block diagram of electronic circuits.

served as monitors. For the beryllium and water absorbers, the front face of each crystal was $25\frac{1}{2}$ in. from the target while, for the Teflon and aluminum absorbers, the distance was reduced to 20 in. A tapered aluminum disk, 1 cm thick, was placed on the front face of each crystal in order to reduce the correction for spurious counts caused by electrons originating in the back end of the absorbers.

A block diagram of the electronics is shown in Fig. 2. Output pulses from the preamplifiers were fed simultaneously into a mixing circuit and into the RIDL Model 30-17 four-channel coincidence and logic circuits. Pulses from the mixing circuit were fed into an RIDL Model 38-12 400-channel analyzer which was subdivided into four quadrants of 100 channels each. Pulses from a given detector were stored in a given quadrant. The four-channel coincidence and logic circuits provided the necessary routing pulses to the 400-channel analyzer. Typical response curves obtained with one of the NaI(Tl) crystals for 20-MeV gamma rays are shown in Fig. 3. The solid curve was obtained in the absence of neutrons from the $T^3(p,n)He^3$ reaction while the broken-line curve illustrates the effect of neutrons from this reaction. The shift in the intercepts is real (the difference in energy of the gamma rays is about 90 keV which corresponds to about $\frac{1}{3}$ of a channel) and is attributed to a change in the gain of the photomultiplier tube in the presence of the intense neutron-induced background of low-energy gamma rays. The change in the peak-to-valley ratio results from pileup and the tail of the 7-MeV capture gamma-ray spectrum from the $I^{127}(n,\gamma)I^{128}$ reaction.

The tritium targets were purchased from the Oak

Ridge National Laboratory and consisted of tritium gas adsorbed in zirconium metal which had been evaporated onto a thin (10-mil) platinum backing. The energy of the gamma rays from the $T^3(p,\gamma)He^4$ reaction is obtained from the conservation laws and is given by

$$E_\gamma = \left[Q + E_p \left(1 - \frac{M_p}{M_\alpha} \right) \right] \left(1 - \frac{Q + E_p [1 - (M_p/M_\alpha)]}{2M_\alpha c^2} \right) \times \left[1 + \frac{M_p}{M_\alpha} \left(\frac{2E_p}{M_p c^2} \right)^{1/2} \cos \Theta \right], \quad (1)$$

where E_p and M_p are the kinetic energy and mass of the proton, M_α is the mass of the He^4 nucleus, Θ is the angle between the emitted photon and the proton beam, and Q is the reaction energy, equal to 19.812 MeV.¹⁰ The energy resolution of the gamma rays is determined primarily by the target thickness and the Doppler width due to the finite angle subtended at the target by the NaI(Tl) crystals. The target thickness is determined experimentally by observing the shape of the $T(p,n)$ yield curve near threshold.¹¹ The Doppler width is obtained by differentiation of Eq. (1) with respect to Θ . The final energy resolution for this experiment is about 40–45 keV.

The aluminum and Teflon absorbers were in the form of machined, truncated cones, 12 and 10 in. long, re-

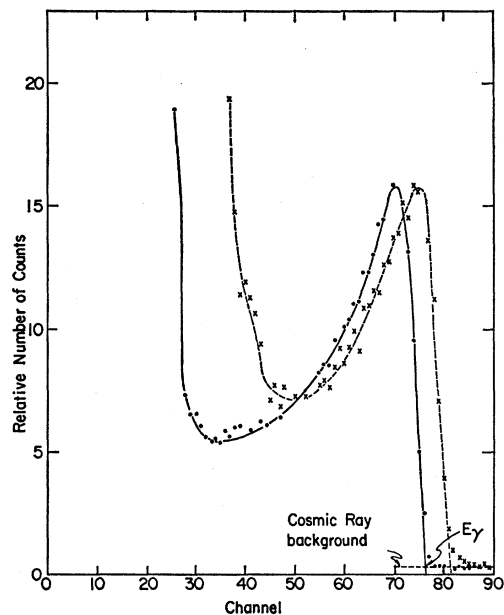


Fig. 3. A response curve of one of the NaI scintillation crystals for 20-MeV gamma rays. The solid-line curve was obtained in the absence of neutrons from the $T^3(p,n)$ reaction in the target. The broken-line curve illustrates the effect of neutrons from this reaction.

¹⁰ F. Everling, L. A. Koenig, J. H. E. Mattuch, and A. H. Wapstra, *Nuclear Data Tables* (U. S. Government Printing Office, Washington, D. C., 1961), Part I.

¹¹ G. A. Jarvis, A. Hemmendinger, H. V. Argo, and R. F. Taschek, *Phys. Rev.* **79**, 929 (1950).

TABLE I. Summary of percent corrections applied.

Absorber	Photon energy (MeV)	Compton photons (%)	Compton electrons (%)	Pair electrons (%)	Pileup (%)	Air absorption (%)	Plexiglas holder (%)
Al	20.41	2.81	0.05	0.006	...	0.06	...
	20.80	2.96	0.06	0.01	0.6	0.06	...
Teflon	20.02	1.53	0.008	0.003	...	0.05	...
	20.50	1.59	0.01	0.005	0.004	0.05	...
Beryllium	20.80	1.65	0.02	0.01	0.004	0.05	...
	20.04	4.50	0.17	0.007	...	0.12	...
Water	20.53	4.76	0.27	0.02	-0.11	0.12	...
	21.02	5.20	0.37	0.03	-0.26	0.12	...
	20.50	2.18	0.29	0.15	-0.07	0.12	-0.71
	21.03	2.35	0.42	0.26	-0.31	0.12	-0.70
	21.52	2.38	0.52	0.35	-0.35	0.12	-0.72
	22.00	2.48	0.65	0.45	-0.37	0.12	-0.79

spectively. The O¹⁶ absorber consisted of distilled water in a plexiglass holder. The holder was in the shape of a truncated cone 24 in. in length. The beryllium absorber was built up using 2-in. cubes (loaned through the courtesy of Dr. Ringo and Argonne National Laboratory) and was 24 in. in length.

The experimental data consisted of sets of response curves, one for each crystal. The number of counts in each crystal was determined by integration of these curves between two fixed points corresponding to 15 MeV and the energy of the gamma ray. As the energy of the gamma rays was obtained by linear extrapolation of the photopeak into background (see Fig. 3), each experimental run provided a new independent calibration of the electronics. The choice of 15 MeV as a lower bias was made in order to reduce the effect of pileup.

For a gamma-ray intensity N_0 , the number of counts in the monitor crystals is $\epsilon_1 N_0 + \beta_1 + P_1$. ϵ_1 is an average efficiency function for the two monitor crystals, β_1 is the cosmic-ray background, and P_1 includes spurious counts due to pileup. The number of counts in the absorber crystals is $\epsilon_2 N_0 e^{-\mu L} + N' + \beta_2 + P_2$, where μ is the attenuation coefficient, L the length of the absorber, and N' the scattered-in counts due to the "bad geometry" of the experiment (discussed below). After subtraction of cosmic-ray background and a suitable pileup correction, the attenuation ratio is

$$R = \epsilon_1 N_0 / (\epsilon_2 N_0 e^{-\mu L} + N') \quad (2)$$

or

$$R = \frac{R_0 N_0}{N_0 e^{-\mu L} + (N'/\epsilon_2)}; \quad R_0 = \frac{\epsilon_1}{\epsilon_2} \quad (3)$$

The "zero" ratio R_0 is determined experimentally by comparing the counting rate in the four crystals with the absorbers removed. The value for ϵ_2 was obtained by an absorption measurement described previously.¹²

CORRECTIONS

In addition to corrections for cosmic-ray background, pileup, and the "bad geometry" of the experiment, the data for each element was corrected for air absorption.

¹² W. Del Bianco and W. E. Stephens, Phys. Rev. **126**, 709 (1962).

TABLE II. Total corrections applied.

Absorber	Photon energy (MeV)	Total correction to the attenuation ratio (%)	μL	Total correction to the total cross section (%)
Aluminum	20.41	2.93	1.814	1.62
	20.80	3.69	1.819	2.03
Teflon	20.02	1.59	0.9517	1.67
	20.50	1.70	0.9369	1.81
Beryllium	20.80	1.77	0.9400	1.88
	20.04	4.80	1.404	3.42
Water ^a	20.53	5.06	1.397	3.62
	21.02	5.46	1.421	3.84
Water ^a	20.50	2.67	1.125	1.66
	21.03	2.84	1.137	1.80
	21.52	3.02	1.112	2.00
	22.00	3.33	1.145	2.12

^a The total correction to the attenuation ratio does not include the correction for the Plexiglas holder. The Plexiglas holder correction is included in the total correction to the cross section.

The oxygen data was corrected for absorption by the plexiglas holder. When calculating cross sections for beryllium, a correction was made for the presence of impurities, since the beryllium blocks consisted of 98.2% Be, 1.7% BeO, and 0.1% Fe.

The scattered-in counts N' come from three sources: (1) Compton-scattered photons; (2) Compton electrons; and, (3) positrons and electrons due to pair production. N' can be written in the form

$$N' = N_0(A_{c\gamma} + A_{ce} + A_{pe}), \quad (4)$$

where $A_{c\gamma}$, A_{ce} , and A_{pe} are constants calculated for each of the three sources of N' .

From Eqs. (3) and (4), the expression for $e^{-\mu L}$ is obtained as

$$e^{-\mu L} = (R_0/R) - (A_{c\gamma} + A_{ce} + A_{pe})/\epsilon_2. \quad (5)$$

The corrections discussed above are tabulated for

TABLE III. Atomic cross sections.

Absorber	Photon energy (MeV)	Compton (mb)	Pair production (mb)	Triplet (mb)	Total (mb)
Aluminum	20.41	387.0	545.1	30.7	962.8
	20.81	381.3	550.3	31.1	962.7
Carbon	20.02	181.3	116.4	13.9	311.6
	20.81	175.9	118.7	14.4	309.0
Fluorine	20.02	272.0	260.3	20.9	553.2
	20.81	263.9	265.5	21.6	551.0
Teflon (CF ₂)	20.02	725.3	637.0	55.7	1418.0
	20.81	703.7	649.7	57.6	1411.0
Beryllium	19.99	121.0	52.0	9.3	182.3
	21.02	116.4	53.4	9.7	179.5
Beryllium (98.2% Be, 1.7% BeO, 0.1% Fe)	19.99	125.5	54.9	9.6	190.0
	21.02	120.7	56.4	10.0	187.1
Hydrogen	20.50	29.7	3.2	2.4	35.3
	22.00	28.1	3.4	2.5	34.0
Oxygen	20.50	237.3	208.6	18.9	464.8
	22.00	224.7	216.0	20.0	460.7
Water	20.50	296.7	215.0	23.7	535.4
	22.00	280.9	222.8	25.0	528.7

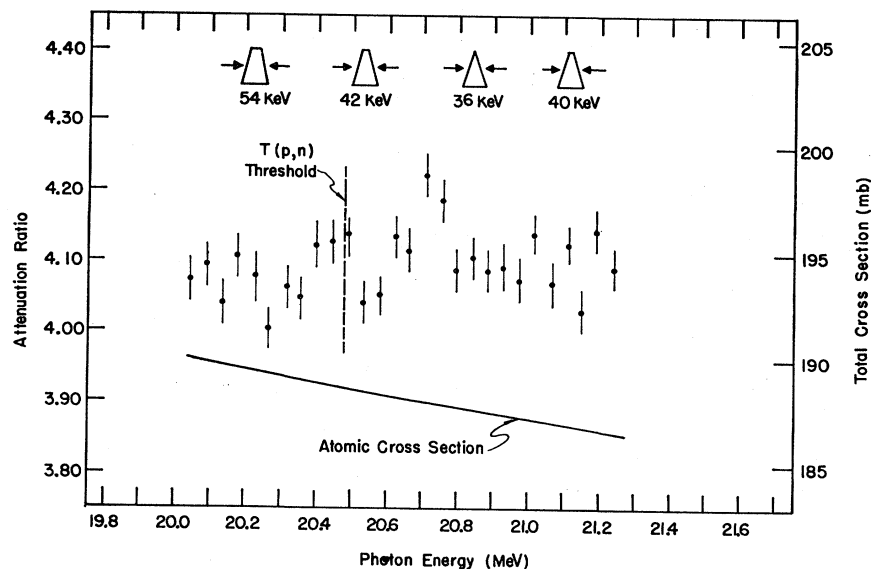


FIG. 4. Attenuation ratio for gamma rays in beryllium as a function of photon energy. The total absorption cross section scale in millibarns is given also. The solid line is the calculated atomic cross section. The trapezoids illustrate the calculated resolution function.

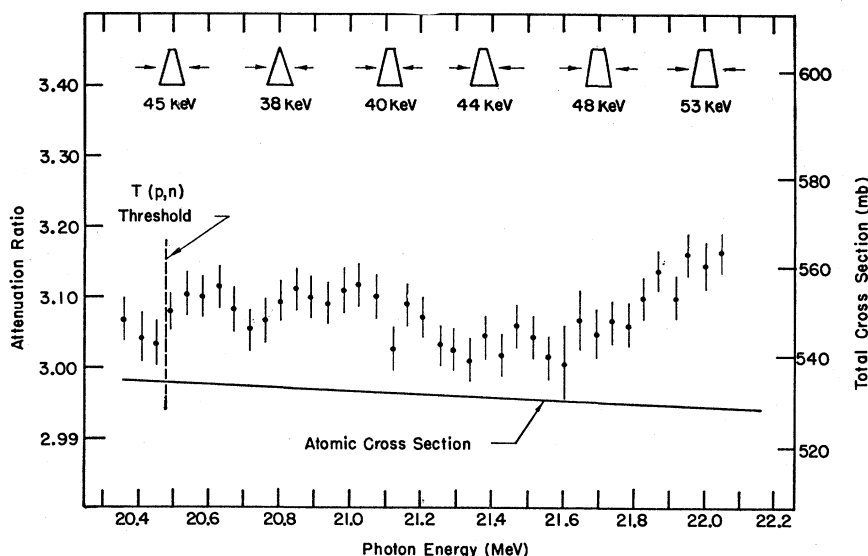


FIG. 5. Attenuation ratio for gamma rays in water as a function of photon energy. The total absorption cross section scale in millibarns is given also. The solid line is the calculated atomic cross section. The trapezoids illustrate the calculated resolution function.

several values of photon energy as percent corrections to the attenuation ratio $e^{-\mu L}$ in Table I. The total corrections applied to the attenuation ratio and the resulting total cross section are summarized for several photon energies in Table II.

ATOMIC CROSS SECTIONS

The desired nuclear absorption is obtained from the total measured absorption cross section by subtracting the theoretical atomic cross sections (Compton effect and pair production). The Compton scattering cross section was calculated using the Klein-Nishina formula for free electrons.¹³ The cross section for pair produc-

tion in the field of the nucleus was calculated from the Bethe-Heitler expression¹⁴ which was obtained using the Born approximation and neglecting screening. A screening correction was deduced from calculations using the Hartree-Fock form factors as given by Nelms and Oppenheim.¹⁵ A small Coulomb correction to the Born approximation (less than 0.2%) was applied to the pair production cross section.¹⁶ The cross section for pair production in the field of an electron was calculated using the integrated cross sections of Borsellino.¹⁷ The

¹⁴ H. Bethe and W. Heitler, Proc. Roy. Soc. (London) **A146**, 83 (1934).

¹⁵ A. T. Nelms and I. Oppenheim, J. Res. Natl. Bur. Std. **55**, 53 (1955).

¹⁶ Dr. H. W. Koch, National Bureau of Standards (private communication).

¹⁷ A. Borsellino, Nuovo, Cimento **4**, 112 (1947); Helv. Phys. Acta **20**, 136 (1947).

¹³ H. A. Bethe and J. Ashkin in *Experimental Nuclear Physics*, edited by E. Segre (John Wiley & Sons, Inc., New York, 1953), Vol. 1, Part II, p. 322.

total atomic cross sections which are the sum of the above contributions are shown on Figs. 4-7 and are tabulated in Table III.

The major uncertainty in the atomic cross sections arises in the calculation of the triplet cross section for pair production in the field of the atomic electrons. The Borsellino value used here does not include screening but is considered to be the most accurate value for light nuclei in this energy region^{16,18} and is assumed to be reliable to about 10%. This causes an uncertainty in the calculated atomic cross sections of 1 mb for Be, 2.4 mb for water, 5.6 mb for Teflon, and 3 mb for Al.

RESULTS

The photonuclear absorption determined by subtracting the calculated atomic cross section from the cor-

TABLE IV. Structure observed in the nuclear absorption cross section curves.

Element	E_{peak} (MeV)	σ_{peak} (mb)	Half-width (MeV)	$\int_{\text{peak}} \sigma dE$ (MeV-mb)
Be ⁹	20.47	6.8	0.13	0.45
	20.73	10.1	0.15	0.9
O ¹⁶	20.62	21.5	0.19	3.9
	21.02 {20.86 21.05}	23.5	~0.40	10.4
F ¹⁹	>22			
	20.09	21.9	0.16	3.5

rected measured total absorption is given in Figs. 8-11. For fluorine, it was necessary also to subtract out the nuclear absorption due to the presence of carbon in the Teflon. The carbon nuclear absorption was obtained from

FIG. 6. Attenuation ratio for gamma rays in teflon as a function of photon energy. The total absorption cross section scale in millibarns is given also. The solid line is the calculated atomic cross section. The trapezoids illustrate the calculated resolution function.

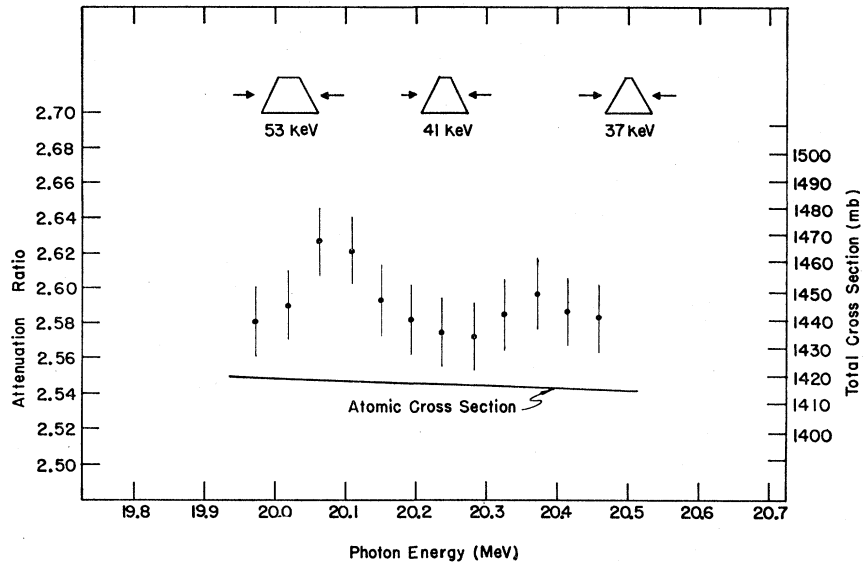
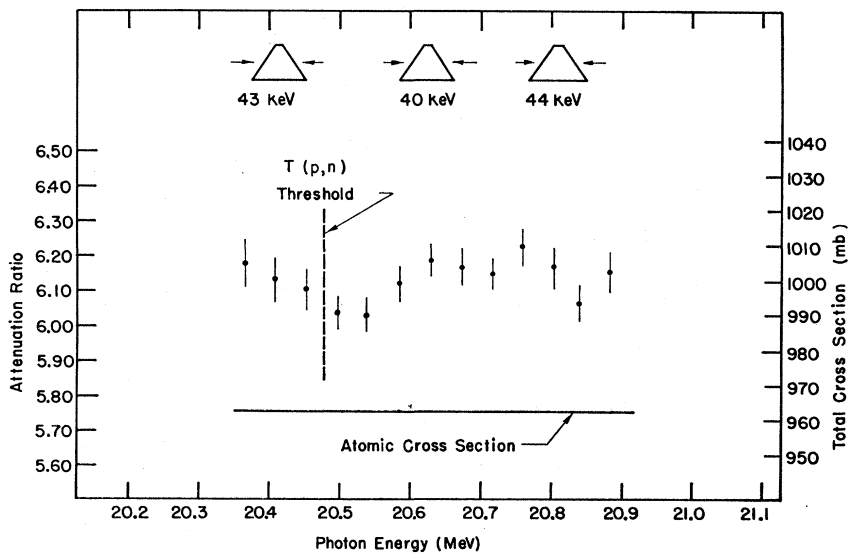


FIG. 7. Attenuation ratio for gamma rays in aluminum as a function of photon energy. The total absorption cross section scale in millibarns is given also. The solid line is the calculated atomic cross section. The trapezoids illustrate the calculated resolution function.



¹⁸ Ch. J. Frei, H. H. Staub, and H. Winkler, *Helv. Phys. Acta* 31, 491 (1958).

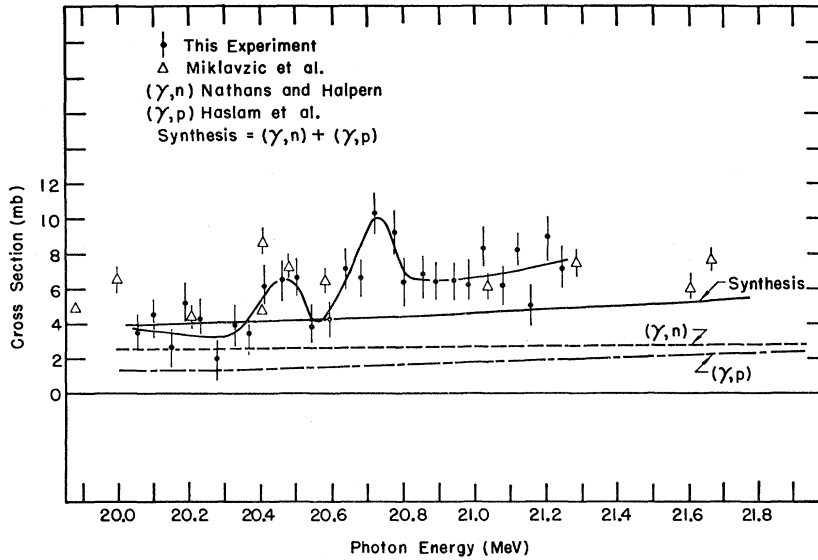


FIG. 8. Nuclear absorption cross section in Be^9 as a function of photon energy. The results of this experiment are plotted as dots. Other results are shown for comparison.

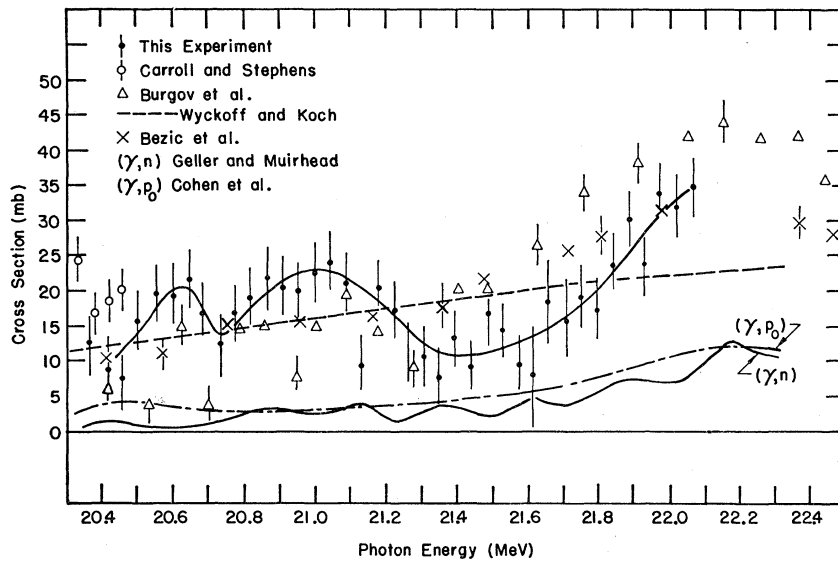


FIG. 9. Nuclear absorption cross section in O^{16} as a function of photon energy. The results of this experiment are plotted as dots. Other results are shown for comparison.

the unpublished measurements of Shin and Stephens on $\text{C}^{12}(\gamma, p)$ and of Geller and Muirhead on $\text{C}^{12}(\gamma, n)$. The flags in the figures represent the relative uncertainty between the points. This uncertainty is mainly due to the statistical uncertainty of the attenuation ratios but is somewhat enlarged by possible errors in the analysis of the response curves. Absolute values are further in error by the uncertainty in the calculated atomic cross sections, in the zero ratio, in the various corrections, and error in density, length and impurities. These absolute errors are estimated to be approximately 1.5 mb for Be, 4 mb for O, 5 mb for F, and 5 mb for Al.

The structure, which appears in these data, is summarized in Table IV. While it is not always clear that these are resolved resonances, they are treated as such in this table.

BERYLLIUM

In Fig. 8 is shown the nuclear absorption in Be^9 as measured in this experiment. For comparison the points reported by Miklavzic *et al.*¹⁹ are plotted on the same graph. They use bremsstrahlung from a 30-MeV betatron and a Compton magnetic spectrometer with an energy resolution of 1.2%. These results are consistent with the present data although the apparent agreement with the peak at 20.7 MeV must be fortuitous since the resolution claimed by Miklavzic was only 0.24 MeV.

The (γ, n) cross section measurements of Nathans and Halpern²⁰ are shown in Fig. 8 as a dashed line. This is

¹⁹ U. Miklavzic, N. Bezic, D. Jamnik, G. Kernel, Z. Milavc, and J. Snajder, Nucl. Phys. **31**, 570 (1962).

²⁰ R. Nathans and J. Halpern, Phys. Rev. **92**, 940 (1953).

FIG. 10. Nuclear absorption cross section in F^{19} as a function of photon energy. The results of this experiment are plotted as dots. Other results are shown for comparison.

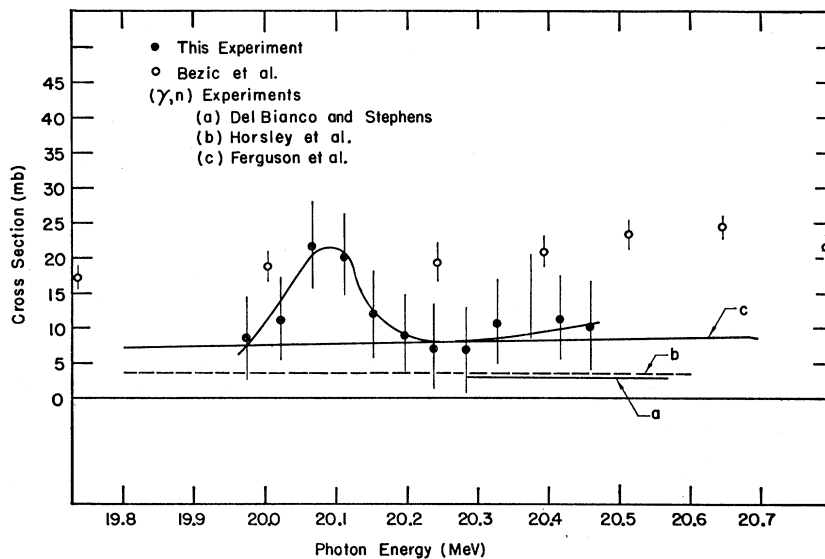
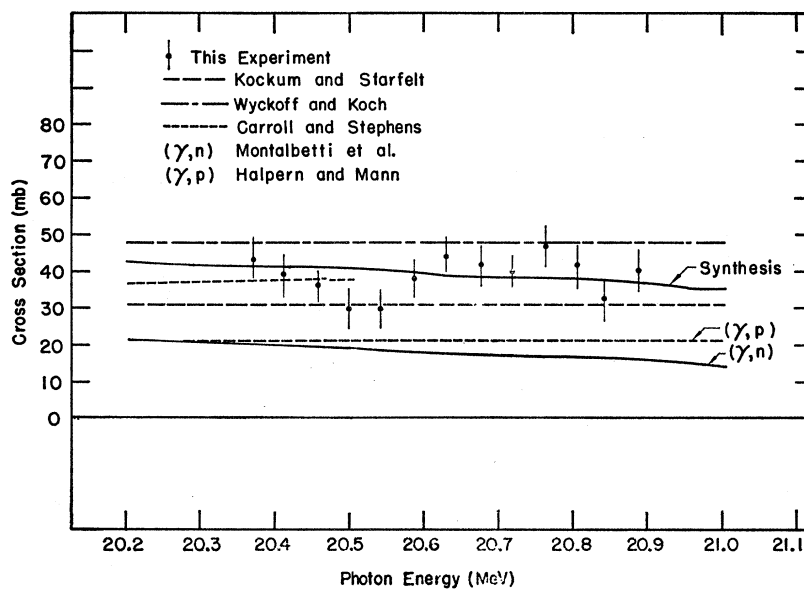


FIG. 11. Nuclear absorption cross section in Al^{27} as a function of photon energy. The results of this experiment are plotted as dots. Other results are shown for comparison.



added to the (γ, p) taken from Haslam *et al.*²¹ to give the synthesized curve also shown in Fig. 8. Not included in this sum are a possible additional few percent of cross section due to (γ, d) and (γ, t) .²² No serious disagreement exists in view of the lack of resolution of the (γ, n) and (γ, p) measurements. Breaks in the $\text{Be}^9(\gamma, p)\text{Li}^8$ beta activity yield curve reported by Stewart²³ at 20.27 and 20.94 MeV do not correspond very well to the structure observed here.

²¹ R. N. H. Haslam, L. Katz, and E. H. Crosby, *Can. J. Phys.* **31**, 210 (1953).

²² B. Cujec, *Nucl. Phys.* **37**, 396 (1962).

²³ M. G. Stewart, Ames Laboratory Research and Development Report IS-191, 1959 (unpublished).

OXYGEN

In Fig. 9 is shown the results of nuclear absorption measurements in oxygen. The solid points with flags are the presently reported data. For comparison, the measurements of Burgov *et al.*²⁴ are shown as triangular points and of Bezic *et al.*²⁵ as crosses. Also indicated is the curve of Wyckoff and Koch²⁶ whose resolution was about 0.5 MeV. The upper curve attempts to represent the trend of our points. In order to allow a comparison

²⁴ N. A. Burgov, G. V. Danilyan, B. S. Dolbilkin, L. E. Lazareva, and F. A. Nikolaev, *Zh. Eksperim. i Teor. Fiz.* **43**, 70 (1962) [English transl.: *Soviet Phys.—JETP* **16**, 50 (1963)].

²⁵ N. Bezic, D. Jamnik, G. Kernel, and J. Snajder (to be published).

²⁶ J. M. Wyckoff and H. W. Koch, *Phys. Rev.* **117**, 1261 (1960).

with the partial cross sections, the data of Geller and Muirhead²⁷ for (γ, n) are drawn together with the (γ, p_0) of Cohen *et al.*²⁸ supported by the (p, γ_0) of Tanner *et al.*²⁹ The sum of the (γ, n) and (γ, p_0) cross sections subtracted from the total absorption cross section would give the expected (γ, p^*) with better accuracy and resolution than that estimated by Fuller and Hayward.³⁰ Our results suggest a relatively large amount of (γ, p^*) in the energy region 20.5–21.2 MeV and an apparent minimum in the region 21.2 to 21.8 MeV with an increase again at higher energies. Selection rules, the group of 2.3-MeV protons observed in the photoproton energy distribution,²⁸ and the large amount of 6.3 gamma rays observed³¹ suggest the favored state for (γ, p^*) to be the $\frac{3}{2}^-$ state at 6.328 MeV in N¹⁵. This large ratio of transitions to the $\frac{3}{2}^-$ state relative to the $\frac{1}{2}^-$ ground state in N¹⁵ seems reasonable in view of the large amount of $P_{3/2}$ hole in theoretically calculated 1⁻ states in this energy region of O¹⁶.³² However, these results place greater emphasis on the $P_{3/2}$ hole at 21 MeV than at 22 MeV while the theoretical calculations reverse this.

The possible peaks at 20.6 and 21 MeV reflect both the (γ, p_0) state at 20.65 MeV^{28,29,33} and the (γ, n_0) states at 20.8 and 21.05 MeV.^{27,34}

FLUORINE

A comparison of the fluorine photoabsorption data is shown in Fig. 10. The present experiment gives results shown by the dots. The data of Bezic *et al.*²⁵ are shown as circles. Measurements of the (γ, n) cross sections are shown in curves a, b, and c in Fig. 10. Curve a gives the results of Del Bianco and Stephens¹² also done with monochromatic gamma rays. The other experiments³⁵ used betatron bremsstrahlung and did not have resolution sufficient to detect variations such as are suggested by the present results.

The present data suggest a peak at 20.09 MeV with characteristics listed in Table IV.

²⁷ K. N. Geller and E. G. Muirhead, Phys. Rev. Letters **11**, 371 (1963).

²⁸ L. D. Cohen, A. K. Mann, B. J. Patton, K. Reibel, W. E. Stephens, and E. J. Winhold, Phys. Rev. **104**, 108 (1956).

²⁹ N. W. Tanner, G. C. Thomas, and E. D. Earle, *Proceedings of the Rutherford Conference*, edited by J. E. Birks (Academic Press Inc., New York, 1961).

³⁰ E. G. Fuller and Evans Hayward, *Nuclear Reactions*, edited by P. M. Endt and P. B. Smith (North-Holland Publishing Company, Amsterdam, 1962), Vol. II.

³¹ N. Svantesson, Bull. Am. Phys. Soc. **1**, 28 (1956).

³² V. Gillet, thesis, Paris, 1962, Rapport CEA No. 2177 (unpublished).

³³ W. R. Dodge and W. C. Barber, Phys. Rev. **127**, 1746 (1962).

³⁴ F. W. K. Firk and K. H. Lokan, Phys. Rev. Letters **8**, 321 (1962).

³⁵ R. J. Horsley, R. N. H. Haslam, and H. E. Johns, Phys. Rev. **87**, 756 (1952). G. A. Ferguson, J. Halpern, R. Nathans, and P. F. Yergin, Phys. Rev. **95**, 776 (1954).

ALUMINUM

The present results for aluminum are shown in Fig. 11 and compared with other data. The agreement with the total absorption measurements of Kockum and Starfelt,³⁶ Wyckoff and Koch³⁷ and Carroll and Stephens⁵ is good. Although the present results have better resolution, no structure is clearly indicated, except for the possibility of a dip at 20.5 MeV.

The (γ, n) results of Montalbetti *et al.*³⁸ and the (γ, p) yield of Halpern and Mann³⁹ are shown in Fig. 11 and added to give a synthesized curve in good agreement with the total absorption.

More recent work on the cross sections shows gross structure with rather wide peaks, but with some discrepancies in position and magnitude. Bolen and Whitehead⁴⁰ indicate a dip in (γ, n) at 20.5 MeV but Mutsuro *et al.*⁴¹ report a peak in (γ, n) at 20.5 MeV and Dular *et al.*⁴² show a peak value of 78 mb in total absorption at 20.4 MeV. These differences may be due to different energy calibration as well as differences in resolution.

CONCLUSION

These results are of value in establishing the total absorption cross sections with an improved accuracy, better resolution and more reliable energy scale than previous measurements. The lack of detailed structure in many cases seems real and not the result of insufficient resolution. The agreement in many cases between total and sum of partial cross sections is encouraging. An extension of these results to a greater range of photon energy would be desirable and may be possible but tedious.

In oxygen the (γ, p_0) and (γ, n) cross sections have been examined with sufficient resolution to allow a deduction of the (γ, p^*) cross section in appreciable detail. The large amount of (γ, p^*) suggested at 21 MeV implies an excess of transition to the $\frac{3}{2}^-$ state of N¹⁵ compared to the $\frac{1}{2}^-$ ground state. While this is in qualitative agreement with the large amount of $1P-\frac{3}{2}$ hole predicted in the wave functions³² of levels in this energy region it seems to give greater emphasis to the $1P-\frac{3}{2}$ hole at 21 MeV than at 22 MeV which reverses the theoretical anticipation.

³⁶ J. Kockum and N. Starfelt, Nuclear Instr. Methods **5**, 37 (1959).

³⁷ J. M. Wyckoff and H. W. Koch, Phys. Rev. **117**, 1261 (1960).

³⁸ R. Montalbetti, L. Katz, and J. Goldemberg, Phys. Rev. **91**, 659 (1953).

³⁹ J. Halpern and A. K. Mann, Phys. Rev. **83**, 370 (1951).

⁴⁰ L. N. Bolen and W. D. Whitehead, Phys. Rev. Letters **9**, 458 (1962).

⁴¹ N. Mutsuro, K. Kageyama, M. Mishina, T. Nakagawa, E. Tanaka, and M. Kimura, J. Phys. Soc. Japan **17**, 1672 (1962).

⁴² J. Dular, G. Kernal, M. Kregar, M. V. Mihailovic, G. Pregl, M. Rosina, and C. Zupancic, Nucl. Phys. **14**, 131 (1959).